

Structural characterization of Fe/TiO<sub>2</sub> nanoparticles: antioxidant and antibacterial studiesMuhammad Arshad<sup>1</sup>, Muhammad Akhyar Farrukh<sup>1,\*</sup>, Raja Adil Sarfraz<sup>2</sup>, Abdul Qayyum<sup>3</sup>, Shaista Ali<sup>1</sup><sup>1</sup>Nano-Chemistry Lab., GC University Lahore-54000, Pakistan<sup>2</sup>Department of Chemistry, University of Agriculture Faisalabad-38040, Pakistan<sup>3</sup>Central Hi-Tech Laboratory, University of Agriculture, Faisalabad 38040, Pakistan

\*corresponding author e-mail address: akhyar100@gmail.com

## ABSTRACT

Iron-Titanium oxide (Fe/TiO<sub>2</sub>) nanoparticles with size from 6.36 to 16.05 nm were prepared by sol-gel method by using acetonitrile, 2-propanol and n-hexane solvents. The synthesized nanomaterial was characterized by X-Ray Diffraction (XRD), Scanning Electron Microscope (SEM), Fourier Transform Infrared (FT-IR), Spectroscopy, Thermogravimetric Analysis (TGA) and Photoluminescence (PL) analysis. Antibacterial activity of the samples was evaluated by using disc diffusion method while antioxidant activity was studied using radical scavenging effect of the 1,1-DiPhenyl-2-Picryl Hydrazyl (DPPH). The Fe/TiO<sub>2</sub> nanoparticles showed the significant antioxidant activity as well as antibacterial activity against both Escherichia coli and Staphylococcus aureus.

**Keywords:** antibacterial; antioxidant; nanoparticles; Fe/TiO<sub>2</sub>; sol-gel method.

## 1. INTRODUCTION

Inhibition of oxidative reactions and study of microbial activity is of great importance in various fields such as pharmaceutical, cosmetic, food and the oxidative stress associated diseases in the human body [1-3].

Demand of new natural antibacterial and antioxidants are increasing tremendously [4] and in this prespective nanoparticles had played an important role [2]. TiO<sub>2</sub> is an important material used for many purposes because of its excellent optical properties and relatively low production cost [5]. Surface photochemistry, high refractive index as well as physical and chemical stability of TiO<sub>2</sub> semiconductor enables multiple application especially for self-cleaning [6], water treatment [7], air purification [8], antibacterial [9, 10], sensors [11], solar energy conversion [12], anti-ultraviolet agent [13, 14], high photo-catalytic activity [15], hydrophilicity [16], and nontoxicity [17, 18]. The catalytic efficiency of TiO<sub>2</sub> depends on number of active sites [18], surface area [19], phase composition [20], and degree of crystallinity [21]. There are three crystalline structures of TiO<sub>2</sub>, rutile [22], anatase [23, 24], and brookite [25]. Rutile is most stable phase [26] and has received increasing attention due to its photocatalytic behavior

[27]. TiO<sub>2</sub> with band gap energy 3.2 eV need UV light source to be photo activated [28] and to improve the band gap of TiO<sub>2</sub>, one of the most effective method involve the doping of metals on TiO<sub>2</sub> [29] such as V [30], Fe [31], Mo [32], Co [33], Au [34] and with nonmetals such as N [35], P [36], S [37] and F [38].

Among all these elements, radius of iron Fe<sup>3+</sup> (0.64 Å) is similar to Ti (0.68 Å) and therefore it is easily doped with TiO<sub>2</sub> [39]. Fe<sup>3+</sup> dopant can serve as charge trap, impeding the electron hole combination rate and enhance photo-catalysis rate [31, 40]. Fe<sup>3+</sup> ions could also combine with -OH group on TiO<sub>2</sub> nanoparticles surface and forms (OH) Fe<sup>3+</sup> complex which is a good source for electron transfer [41]. Sol-gel [24, 42], hydrothermal [43], and wet chemical synthesis [44] are well known methods for synthesis of nanoparticles and could be used to synthesize Fe/TiO<sub>2</sub> nanoparticles.

In this work Fe/TiO<sub>2</sub> nanoparticles were synthesized at low temperature by sol-gel method. The aim of present work was to study the effect of Fe doping on photoluminescence and antibacterial and antioxidant behavior of synthesized TiO<sub>2</sub> nanoparticles.

## 2. EXPERIMENTAL SECTION

## 2.1. Materials.

Iron chloride hexa-hydrate (FeCl<sub>3</sub>.6H<sub>2</sub>O) and acetonitrile were purchased from Merck, Tartaric acid, n-hexane and 2-propanol were purchased from Fisher, Nitric acid (HNO<sub>3</sub>) and Titanium isopropoxide were purchased from Sigma Aldrich. All the chemicals were of analytical grade and were used without further purification.

## 2.2. Apparatus.

Fourier Transform Infrared (FTIR) spectroscopy was done to confirm the presence of functional groups of metal oxide by using Prestige-21, X-ray diffraction (XRD) characterization was

carried out to observe crystallite shape using X'Pert PRO, Thermogravimetry analysis (TGA) was done using G600 V8.3 Build, Morphology of nanoparticles were observed using Scanning Electron Microscope (SEM) on Hitachi S3400N at an accelerating voltage of 15.0 and 20.0 kV. Photoluminescence (PL) Analysis was done to observe the band gap of nanoparticles using Hitachi F-7000.

2.3. Preparation of Fe doped TiO<sub>2</sub> nanoparticles.

20 mL of acetonitrile and 10 mL of titanium isopropoxide were stirred for twenty minutes at room temperature. 0.1 M solution of iron chloride (0.540g / 20 mL of acetonitrile) was

added in the above prepared solution. Concentrated HNO<sub>3</sub> was added drop wise to form acidic media as hydrolysis catalyst. The mixture was transparent at this condition. 4.0 M liquid ammonia was added drop wise until the pH reached 6.2 then solution was stirred for 4 hours on hotplate at 75 °C and later centrifuged at 2500 rpm for 30 minutes. The precipitates were separated and washed several times with water and ethanol and dried at 80°C for 3 hours and then calcined at 700 °C for 3 hours. Same procedure was repeated for the synthesis of Fe/TiO<sub>2</sub> nanoparticles by using solvents with same molar concentration.

#### 2.4. Antibacterial activity.

Antibacterial activity of Fe/TiO<sub>2</sub> nanoparticles were studied against two bacterial strains; Escherichia coli and Staphylococcus aureus.

Bacterial growth medium, cultures and inoculums preparation was done by taking 13 g of nutrient broth (Oxoid) and mix in 1000 mL distilled water and distributed homogenously. The medium was autoclaved at 121 °C for 15 minutes. Loop full of pure culture of a bacterial strain was mixed in the medium and placed in shaker for 24 hours at 37 °C. The inoculums were stored at 4 °C. The inoculums with 1×10<sup>8</sup> spores / mL were used for further analysis.

Antibacterial assay for disc diffusion method was prepared by taking Nutrient agar (Oxoid) 28 g mixed in 1000 mL distilled water, distributed homogeneously and medium was sterilized by autoclaving at 121 °C for 15 min. Before the medium was

transferred to sterilized petri plates; inoculation (100 µL/100 mL) was added to the medium and poured in sterilized petri plates. After this, small filter paper discs were laid flat on growth medium containing 100 µL of Fe/TiO<sub>2</sub> nanoparticles.

The petri plates were then incubated at 37 °C for 24 hours, for the growth of bacteria. The nanoparticles inhibited the bacterial growth and clear zones were formed. The zones of inhibition were measured in millimeters using zone reader [45].

#### 2.5. Determination of antioxidant activity by DDPH free radical scavenging assay.

Antioxidant activity of nanoparticles and the standard were evaluated on the basis of the radical scavenging effect of the stable 1,1-DiPhenyl-2-Picryl Hydrazyl (DPPH) free radical activity by modified method [46, 47].

Solution of Fe/TiO<sub>2</sub> nanoparticles, ascorbic acid (standard) and DPPH were prepared in n-hexane. 2 mL of 0.002 % solution of DPPH was mixed with 2 mL of sample solution of each dilution separately. These solution mixtures were kept in dark for 30 minutes and the absorbance was observed at maximum wavelength (517 nm). n-hexane solvent was used as blank and absorbance was recorded, percentage inhibition was calculated using the formula as given below:

$$I \% = (A_{\text{blank}} - A_{\text{sample}} / A_{\text{blank}}) \times 100$$

Where A<sub>blank</sub> is the absorbance of the standard (containing all reagents except the test compound) and A<sub>sample</sub> is the absorbance of the test compound.

### 3. RESULTS SECTION

#### 3.1. Characterization.

##### 3.1.1. FT-IR.

Figure 1(a) and (b) showed the FTIR spectra of TiO<sub>2</sub> and Fe /TiO<sub>2</sub> nanoparticles, peaks obtain at 3412 and 3419 cm<sup>-1</sup> were due to stretching vibration of -OH [48]. The peaks at 1631 and 1625 cm<sup>-1</sup> are related to the bending vibration of -OH [49]. The peaks at 1047, 1056 [4] and 426 cm<sup>-1</sup> [48] were due to stretching vibration of Ti-O. A peak at 563 cm<sup>-1</sup>[50] of Fe was observed in Figure 1 (b), confirms the formation of Fe/TiO<sub>2</sub> nanoparticles.

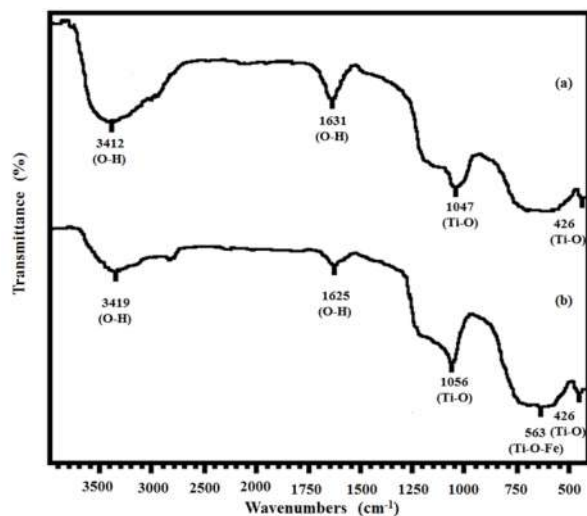


Figure 1. FTIR Spectra of (a) TiO<sub>2</sub> (b) Fe/TiO<sub>2</sub> nanoparticles.

##### 3.1.2. XRD Analysis.

The phase composition and the crystallite size of the TiO<sub>2</sub> and Fe/TiO<sub>2</sub> were evaluated by X-ray diffraction analysis as shown in Figure 2 and 3. XRD pattern in Figure 2 shows tetragonal shape of Rutile TiO<sub>2</sub>. The essential peaks of pure TiO<sub>2</sub> nanoparticles are present at 2θ degrees of 27.46, 36.05, 41.22, 44.05, 54.33, 56.63, 62.72, 64.03 and 69.76° with planes of (110), (101), (111), (210), (211), (220), (002), (310) and (112) respectively, which are all well indexed with PDF # 00-004-0551. Figure 3 shows the XRD patterns of Fe/TiO<sub>2</sub> nanoparticles synthesized using acetonitrile (Figure 3a), 2-propanol (Figure 3b) and n-hexane (Figure 3c). After Fe doping, the typical position of TiO<sub>2</sub> at (101) shifts to a larger angle indicating presence of Fe. Fe/TiO<sub>2</sub> nanoparticles showed characteristics peaks at 2θ = 32.5, 33.2, 35.96, 41.01, 43.67, 49.26, 54.35, 56.61, 62.78, 63.96 and 69.37° with diffraction planes (101), (104), (110), (021), (202), (024), (116), (018), (027), (300), and (208) respectively [51].

Average crystallite size of TiO<sub>2</sub> was calculated by using the Scherrer's equation (Eq. 1)

$$D = k\lambda / (\beta \cos \theta) \quad \text{Eq.1}$$

D is the average crystallite size, β is the broadening of peak at half the maximum intensity in radians. λ wavelength of incident radiations in nm, k is the grain shape dependent constant (k = 0.89) and θ is diffraction angle.

The average size of TiO<sub>2</sub> was found 34 nm and of Fe/TiO<sub>2</sub> nanoparticles was calculated as 6.36 nm in acetonitrile, 9.42 nm in

2-propanol, and 16.05 nm in n-hexane. The particle size of TiO<sub>2</sub> nanoparticles was observed decreased by doping of Fe on TiO<sub>2</sub>.

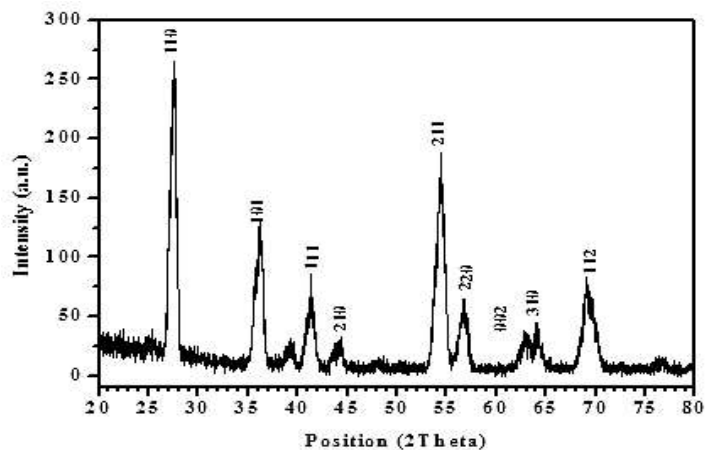


Figure 2. XRD Spectra of TiO<sub>2</sub> nanoparticles.

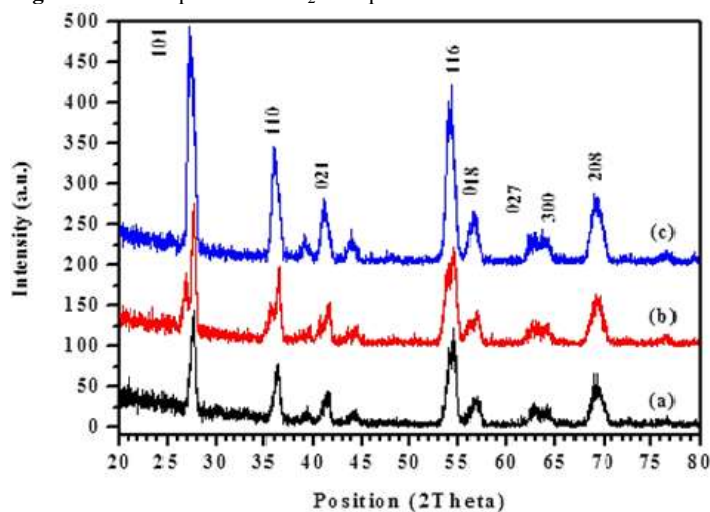


Figure 3. XRD patterns of Fe-doped TiO<sub>2</sub> using (a) acetonitrile (b) 2-propanol (c) n-hexane.

### 3.1.3. SEM Analysis.

Figure 4 shows the SEM image of Fe/TiO<sub>2</sub> nanoparticles are inter-connected, spherical and have porous surface morphology.

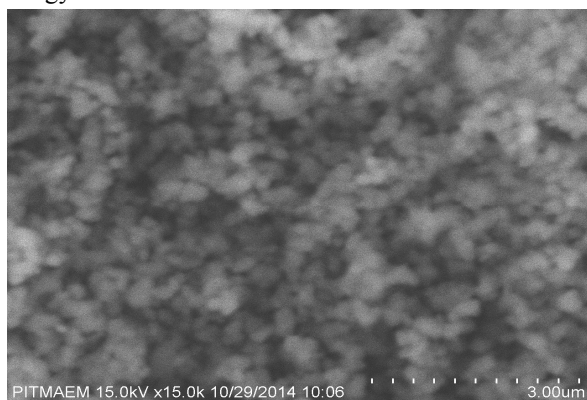


Figure 4. SEM image of Fe-TiO<sub>2</sub> nanoparticles.

### 3.1.4. TGA Analysis.

Figure 5 shows the TGA-DSC curves of uncalcined Fe/TiO<sub>2</sub> nanoparticles. A small endothermic peak at 75 °C is due to water loss and exothermic peak at 230 °C is attributed to the thermal decomposition of the organic matter present during

synthesis. Mass loss about 12 % up to 490 °C was observed due to removal of H<sub>2</sub>O, OH<sup>-</sup>.

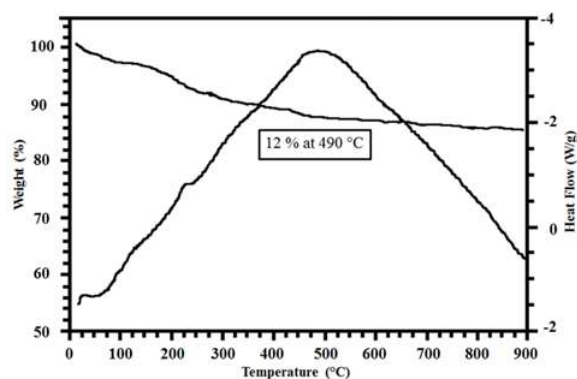


Figure 5. TGA-DSC graph of Fe/TiO<sub>2</sub>.

### 3.1.5. Photoluminescence Analysis.

Figure 6 shows the photoluminescence spectra of Fe/TiO<sub>2</sub> nanoparticles having two distinct emission peaks, one in sharp UV region and other in broad visible green region. Fe/TiO<sub>2</sub> gives the spectral bands at 355-450 nm which should be ascribed to self-trapped excitons and oxygen vacancies [13] respectively. The band gap observed using equation 2 was 2.75 eV which is much lower than reported in literature (3.27 eV) [52].

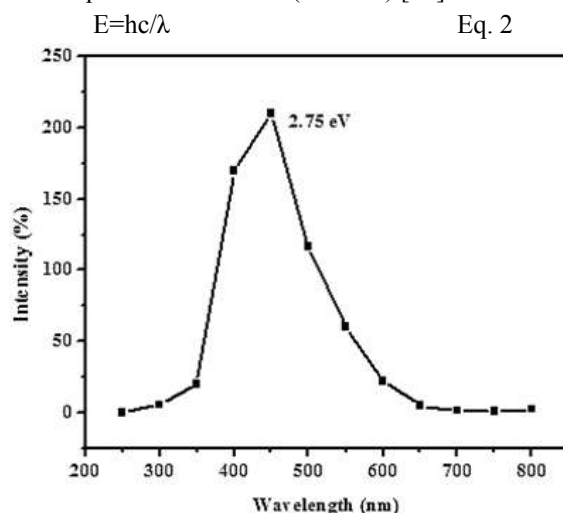
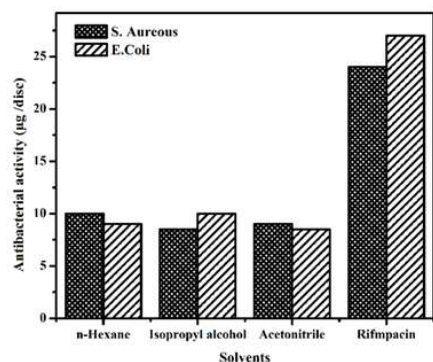


Figure 6. PL-Spectra of Fe/TiO<sub>2</sub> nanoparticles.

### 3.2. Antibacterial activity of Fe/TiO<sub>2</sub>.

The antibacterial activity of Fe/TiO<sub>2</sub> synthesized using different solvents such as acetonitrile, 2-propanol and n-hexane was investigated against strains of gram positive bacteria (*S. aureus*) and gram negative bacteria (*E. coli*) and the standard Rifampicin was also tested. The results of gram positive bacteria *S. aureus* using disc diffusion method showed that the nanoparticles synthesized in n-hexane showed the highest inhibition 10 µg/disc followed by 9 µg/disc inhibition nanoparticles synthesized in acetonitrile. While the lowest inhibition 8.5 µg/disc was shown by the nanoparticles synthesized in 2-propanol and standard antibacterial agents Rifampicin showed the 24 µg/disc inhibition.

The inhibition activity of these particles was also performed against gram negative bacteria *E. Coli* which showed highest inhibition 10 µg/disc by the particles synthesized in 2-propanol solvent followed 9 µg/disc by n-hexane solvents.



**Figure 7.** Antibacterial activity of Fe/TiO<sub>2</sub> nanoparticles in different solvents (Rifampicin is a standard antibacterial agent).

The particles synthesized in acetonitrile showed the lowest inhibition 8.5 µg /disc against the gram negative bacteria (Table 1)

**Table 1.** Antibacterial and Antioxidant activity of Fe/TiO<sub>2</sub> nanoparticles.

Sr. No.	Solvents	XRD Crystallite Size (nm)	Anti-bacterial activity		Anti-oxidant activity (%)
			gram +ve (µg)	gram -ve (µg)	
1	Acetonitrile	6.36	9	8.5	20.17
2	2-propanol	9.42	8.5	10	21.61
3	n-hexane	16.05	10	9	25.34

#### 4. CONCLUSIONS

Synthesis of Fe/TiO<sub>2</sub> nanoparticles by sol-gel method was carried out in three different solvents acetonitrile, 2-propanol and n-hexane. The results showed that crystallite size decreases from 6.36 nm to 16.05 nm and band gap also decreases from 3.27 to 2.75 eV. The antibacterial activity by using disc diffusion method revealed that nanoparticles synthesized in n-hexane showed

while the standard showed the highest 27 µg /disc inhibition which is greater than the all particles as shown in Figure 7. The results revealed overall inhibition against both gram positive and negative bacteria but less than the standard used.

#### 3.3. Antioxidant activity of Fe/TiO<sub>2</sub>.

The antioxidant activity of Fe/TiO<sub>2</sub> was investigated by DPPH scavenging assay using ascorbic acid as standard. The results obtained were represented in Table 1. Nanoparticles synthesized in n-hexane shows highest scavenging activity 25.34 % followed by 2-propanol 21.61 % and acetonitrile showed the lowest inhibition 20.17 %. The ascorbic acid in n-hexane showed the highest activity 73.54 %. Table 1 showed that by changing solvent crystallite size increase and the antioxidant activity of Fe/TiO<sub>2</sub> nanoparticles increases.

highest inhibition in gram +ve bacteria while nanoparticles synthesized in 2-propanol showed highest inhibition in gram -ve bacteria. The antioxidant activity of nanoparticles by DPPH assay showed that by increasing crystallite size of nanoparticles, DPPH scavenging activity increases from 20.17 to 25.34 %.

#### 5. REFERENCES

- [1] Aksoy L., Kolay E., Ağılönü Y., Aslan Z., Kargioğlu M., Free radical scavenging activity, total phenolic content, total antioxidant status, and total oxidant status of endemic Thermopsis turcica, *Saudi Journal of Biological Sciences*, 20, 235-239, **2013**.
- [2] Hajipour M.J., Fromm K.M., Ashkarran A.A., Aberasturi D.J.D, Larramendi I.R.D., Rojo T., Serpooshan V., Parak W.J., Mahmoudi M., Antibacterial properties of nanoparticles, *Trends in Biotechnology*, 30, 499-511, **2012**.
- [3] Cardona F., Andrés-Lacueva C., Tulipani S., Tinahones F.J., Queipo-Ortuño M.I., Benefits of polyphenols on gut microbiota and implications in human health, *The Journal of Nutritional Biochemistry*, 24, 1415-1422, **2013**.
- [4] Lopez E.S.T., Bosch P., Meas Y., Gomez R., FTIR and UV-Vis (diffuse reflectance) spectroscopic characterization of TiO<sub>2</sub> sol-gel, *Materials Chemistry and Physics*, 32, 141-152, **1992**.
- [5] Park Y.R., Kim K.J., Structural and optical properties of rutile and anatase TiO<sub>2</sub> thin films: Effects of Co doping, *Thin Solid Films*, 484, 34-38, **2005**.
- [6] Carneiro J.O., Teixeira V., Portinha A., Magalhães A., Coutinho P., Tavares C.J., Newton R., Iron-doped photocatalytic TiO<sub>2</sub> sputtered coatings on plastics for self-cleaning applications, *Materials Science and Engineering: B*, 138, 144-150, **2007**.
- [7] Lachheb H., Puzenat E., Houas A., Ksibi M., Elaloui E., Guillard C., Herrmann J.M., Photocatalytic degradation of various types of dyes (Alizarin S, Crocein Orange G, Methyl Red, Congo Red, Methylene Blue) in water by UV-irradiated titania, *Applied Catalysis B: Environmental*, 39, 75-90, **2002**.
- [8] Wang S., Yu H., Cheng X., Degradation of Typical Indoor Air Pollutants Using Fe-Doped TiO<sub>2</sub> Thin Film under Daylight Illumination, *Journal of Chemistry*, 2014, 5, **2014**.
- [9] Huijun Z., Hongmei L., Changsheng M., Chengjun Q., Dajun W., Antibacterial Properties of Nanometer Fe<sup>3+</sup>-TiO<sub>2</sub> Thin Films, in: Nano/Micro Engineered and Molecular Systems, 2006.NEMS '06. 1st IEEE International Conference on, 955-958, **2006**.
- [10] Naseem T., Farrukh M. A., Antibacterial Activity of Green Synthesis of Iron Nanoparticles Using Lawsonianermis and Gardenia jasminoides Leaves Extract., *Journal of Chemistry*, 7, **2015**.
- [11] Rella R., Spadavecchia J., Manera M.G., Capone S., Taurino A., Martino M., Caricato A.P., Tunno T., Acetone and ethanol solid-state gas sensors based on TiO<sub>2</sub> nanoparticles thin film deposited by matrix assisted pulsed laser evaporation, *Sensors and Actuators B: Chemical*, 127, 426-431, **2007**.
- [12] Jung H.S., Lee J.K., Nastasi M., Lee S.W., Kim J.Y., Park J.S., Hong K.S., Shin H., Preparation of Nanoporous MgO-Coated TiO<sub>2</sub> Nanoparticles and Their Application to the Electrode of Dye-Sensitized Solar Cells, *Langmuir*, 21, 10332-10335, **2005**.
- [13] Hoffmann M.R., Martin S.T., Choi W., Bahnemann D.W., Environmental Applications of Semiconductor Photocatalysis, *Chemical Reviews*, 95, 69-96, **1995**.
- [14] Fujishima A., Honda K., Electrochemical Photolysis of Water at a Semiconductor Electrode, *Nature*, 238, 37-38, **1972**.
- [15] Tachikawa T., Takai Y., Tojo S., Fujitsuka M., Irie H., Hashimoto K., Majima T., Visible Light-Induced Degradation of Ethylene Glycol on Nitrogen-Doped TiO<sub>2</sub> Powders, *The Journal of Physical Chemistry B*, 110, 13158-13165, **2006**.
- [16] Thompson T.L., Yates J.T., Surface Science Studies of the Photoactivation of TiO<sub>2</sub>, *New Photochemical Processes, Chemical Reviews*, 106, 4428-4453, **2006**.
- [17] Hsien Y.H., Chang C.F., Chen Y.H., Cheng S., Photodegradation of aromatic pollutants in water over TiO<sub>2</sub> supported on molecular sieves, *Applied Catalysis B: Environmental*, 31, 241-249, **2001**.
- [18] Huang J.H., Li C.P., Chang-Jian C.W., Lee K.C., Huang J.H., Preparation and characterization of high refractive index silicone/TiO<sub>2</sub>nanocomposites for LED encapsulants, *Journal of the Taiwan Institute of Chemical Engineers*, 46, 168-175, **2015**.
- [19] Xiong S., Tang Y., Ng H.S., Zhao X., Jiang Z., Chen Z., Ng K.W., Loo S.C.J., Specific surface area of titanium dioxide (TiO<sub>2</sub>) particles influences cyto- and photo-toxicity, *Toxicology*, 304, 132-140, **2013**.

- [20] Molinari A., Bonino F., Magnacca G., Demaria F., Maldotti A., Relation between phase composition and photocatalytic activity of TiO<sub>2</sub> in a sulfoxidedeoxygenation reaction, *Materials Chemistry and Physics*, 158, 60-66, **2015**.
- [21] Kim D.S., Kwak S.Y., The hydrothermal synthesis of mesoporous TiO<sub>2</sub> with high crystallinity, thermal stability, large surface area, and enhanced photocatalytic activity, *Applied Catalysis A: General*, 323, 110-118, **2007**.
- [22] Zhu H.X., Zhou P.X., Li X., Liu J.M., Electronic structures and optical properties of rutile TiO<sub>2</sub> with different point defects from DFT calculations, *Physics Letters A*, 378, 2719-2724, **2014**.
- [23] Sugimoto T., Zhou X., Muramatsu A., Synthesis of uniform anatase TiO<sub>2</sub> nanoparticles by gel-sol method: 3. Formation process and size control, *Journal of Colloid and Interface Science*, 259, 43-52, **2003**.
- [24] Javaid S., Farrukh M.A., Muneer I., Shahid M., Khaleeq-ur-Rahman M., Umar A.A., Influence of optical band gap and particle size on the catalytic properties of Sm/SnO<sub>2</sub>-TiO<sub>2</sub> nanoparticles, *Superlattices and Microstructures*, 82, 234-247, **2015**.
- [25] Lee B.I., Wang X., Bhave R., Hu M., Synthesis of brookite TiO<sub>2</sub> nanoparticles by ambient condition sol process, *Materials Letters*, 60, 1179-1183, **2006**.
- [26] Dyk A.C.V., Heyns A.M., Dispersion Stability and Photo-activity of Rutile (TiO<sub>2</sub>) Powders, *Journal of Colloid and Interface Science*, 206, 381-391, **1998**.
- [27] Wang C., Shao C., Liu Y., Li X., Water-Dichloromethane Interface Controlled Synthesis of Hierarchical Rutile TiO<sub>2</sub> Superstructures and Their Photocatalytic Properties, *Inorganic Chemistry*, 48, 1105-1113, **2009**.
- [28] Xu T.H., Song C.L., Liu Y., Han G.R., Band structures of TiO(2) doped with N, C and B, *Journal of Zhejiang University. Science. B*, 7, 299-303, **2006**.
- [29] Dong Y., Kapilashrami M., Zhang Y., Guo J., Morphology change and band gap narrowing of hierarchical TiO<sub>2</sub> nanostructures induced by fluorine doping, *CrystEngComm*, 15, 10657-10664, **2013**.
- [30] Tsuyumoto I., Nawa K., Thermochromism of vanadium-titanium oxide prepared from peroxovanadate and peroxotitanate, *Journal of Material Science*, 43, 985-988, **2008**.
- [31] Naeem K., Ouyang F., Preparation of Fe<sup>3+</sup>-doped TiO<sub>2</sub> nanoparticles and its photocatalytic activity under UV light, *Physica B: Condensed Matter*, 405, 221-226, **2010**.
- [32] Du Y.K., Gan Y.Q., Yang P., Zhao F., Hua N.P., Jiang L., Improvement in the heat-induced hydrophilicity of TiO<sub>2</sub> thin films by doping Mo(VI) ions, *Thin Solid Films*, 491, 133-136, **2005**.
- [33] Sarkar D., Ghosh C.K., Maiti U.N., Chattopadhyay K.K., Effect of spin polarization on the optical properties of Co-doped TiO<sub>2</sub> thin films, *Physica B: Condensed Matter*, 406, 1429-1435, **2011**.
- [34] Li H., Bian Z., Zhu J., Huo Y., Li H., Lu Y., Mesoporous Au/TiO<sub>2</sub> Nanocomposites with Enhanced Photocatalytic Activity, *Journal of the American Chemical Society*, 129, 4538-4539, **2007**.
- [35] Shang G., Fu H., Yang S., Xu T., Mechanistic Study of Visible-Light-Induced Photodegradation of 4-Chlorophenol by TiO<sub>2</sub> with Low Nitrogen Concentration, *International Journal of Photoenergy*, 9, **2012**.
- [36] Lv Y., Yu L., Huang H., Liu H., Feng Y., Preparation, characterization of P-doped TiO<sub>2</sub> nanoparticles and their excellent photocatalytic properties under the solar light irradiation, *Journal of Alloys and Compounds*, 488, 314-319, **2009**.
- [37] Umebayashi T., Yamaki T., Itoh H., Asai K., Band gap narrowing of titanium dioxide by sulfur doping, *Applied Physics Letters*, 81, 454-456, **2002**.
- [38] Dozzi M.V., Livraghi S., Giamello E., Selli E., Photocatalytic activity of S- and F-doped TiO<sub>2</sub> in formic acid mineralization, *Photochemical & Photobiological Sciences*, 10, 343-349, **2011**.
- [39] Zhou M., Yu J., Cheng B., Effects of Fe-doping on the photocatalytic activity of mesoporous TiO<sub>2</sub> powders prepared by an ultrasonic method, *Journal of Hazardous Materials*, 137, 1838-1847, **2006**.
- [40] Zhang Y., Shen Y., Gu F., Wu M., Xie Y., Zhang J., Influence of Fe ions in characteristics and optical properties of mesoporous titanium oxide thin films, *Applied Surface Science*, 256, 85-89, **2009**.
- [41] Wang J., Liu Z., Cai R., A New Role for Fe<sup>3+</sup> in TiO<sub>2</sub> Hydrosol: Accelerated Photodegradation of Dyes under Visible Light, *Environmental Science & Technology*, 42, 5759-5764, **2008**.
- [42] Perveen H., Farrukh M.A., Khaleeq-ur-Rahman M., Munir B., Tahir M.A., Synthesis, structural properties and catalytic activity of MgO-SnO<sub>2</sub> nanocatalysts, *Russian Journal of Physical Chemistry*, 89, 99-107, **2015**.
- [43] Ali S., Farrukh M.A., Khaleeq-ur-Rahman M., Photodegradation of 2,4,6-trinitrophenol catalyzed by Zn/MgO nanoparticles prepared in aqueous-organic medium, *Korean Journal Chemical Engineering*, 30, 2100-2107, **2013**.
- [44] Wang C.Y., Botcher C., Bahnmann D.W., Dohrmann J.K., A comparative study of nanometer sized Fe(III)-doped TiO<sub>2</sub> photocatalysts: synthesis, characterization and activity, *Journal of Materials Chemistry*, 13, 2322-2329, **2003**.
- [45] Afzal M.S.M., Jamil A., Rehman S.U., Phytochemical spectrum of essential oil of Paganumharmala by GC-MS and antimicrobial activity using sequential solvents fractions and essential oils, *Asian Journal of Chemistry*, 26, 574-578, **2014**.
- [46] Mimica-Dukić N., Bozin B., Soković M., Mihajlović B., Matavulj M., Antimicrobial and antioxidant activities of three Mentha species essential oils, *Plantamedica*, 69, 413-419, **2003**.
- [47] Jain R., Jain S.K., Total phenolic contents and antioxidant activities of some selected anticancer medicinal plants from chhattisgarh state India., *Pharmacologyonline*, 2, 755-762, **2011**.
- [48] Kumar P.M., Badrinarayanan S., Sastry M., Nanocrystalline TiO<sub>2</sub> studied by optical, FTIR and X-ray photoelectron spectroscopy: correlation to presence of surface states, *Thin Solid Films*, 358, 122-130, **2000**.
- [49] Liu P., Borrell P.F., Božič M., Kokol V., Oksman K., Mathew A.P., Nanocelluloses and their phosphorylated derivatives for selective adsorption of Ag<sup>+</sup>, Cu<sup>2+</sup> and Fe<sup>3+</sup> from industrial effluents, *Journal of Hazardous Materials*, 294, 177-185, **2015**.
- [50] Moretti R., Arienzo I., Civetta L., Orsi G., Papale P., Multiple magma degassing sources at an explosive volcano, *Earth and Planetary Science Letters*, 367, 95-104, **2013**.
- [51] Nasralla N., Yeganeh M., Astuti Y., Piticharoenphun S., Shahtahmasebi N., Kompany A., Karimipour M., Mendis B.G., Poolton N.R.J., Šiller L., Structural and spectroscopic study of Fe-doped TiO<sub>2</sub> nanoparticles prepared by sol-gel method, *ScientiaIranica*, 20, 1018-1022, **2013**.
- [52] Gharagozlu S.N.M., Preparation of vitamin B<sub>12</sub>-TiO<sub>2</sub> nano hybrid studied by TEM, FTIR and optical analysis techniques, *Materials Science in Semiconductor Processing*, 35, 166-173, **2015**.

## 6. ACKNOWLEDGEMENTS

The principal investigator (Muhammad Akhyar Farrukh) of projects would like to thank The World Academy of Sciences (TWAS) (research grant number 11-028 RG/MSN/AS\_C) and Higher Education Commission (HEC) Pakistan (grant number 20-2660/NRPU/R&D/HEC/13) for establishing nanochemistry lab to conduct this research work.

© 2016 by the authors. This article is an open access article distributed under the terms and conditions of the Creative Commons Attribution license (<http://creativecommons.org/licenses/by/4.0/>).